Journal of Sound and Vibration (2002) **253**(2), 329–345
doi:10.1006/jsvi.2001.3813, available online at http://www.idealibrary.com on IDEAL®

VIBRATION OF PLATES IN DIFFERENT SITUATIONS USING A HIGH-PRECISION SHEAR DEFORMABLE ELEMENT

A. H. SHEIKH

Department of Ocean Engineering and Naval Architecture, Indian Institute of Technology, Kharagpur 721 302, *India. E-mail*: *hamid@naval.iitkgp.ernet.in*

AND

S. HALDAR AND D. SENGUPTA

Department of Applied Mechanics, Bengal Engineering College (*Deemed University*), *Howrah* 711 103, *India*

(*Received* 12 *July* 2000, *and in final form* 26 *March* 2001)

A high-precision thick plate element proposed by the last author of this paper has been applied to free vibration analysis of plates to study its performance. The element has a triangular shape and it has three nodes at its corners, three mid-side nodes on each side and four nodes within the element. The transverse displacement and rotations of the normal have been taken as independent field variables and they have been approximated with polynomials of different orders. This has not only helped to include the effect of shear deformation but also made the element free from locking in shear. Initially, the number of degrees of freedom of the element is 35, which is reduced to 30 by eliminating the degrees of freedom of the internal nodes. This has been done through static condensation. To facilitate the condensation process, efficient mass lumping schemes have been recommended to form the mass matrix having zero mass for the internal nodes. Recommendation has also been made for the inclusion of mass for rotary inertia in a lumped mass matrix. Numerical examples of plates having different shapes and boundary conditions have been solved by this element. Examples of plates having internal cutout and concentrated mass have also been studied. The results obtained in all the cases have been compared with the published results to show the accuracy and range of applicability of the present element.
© 2002 Elsiver Science Ltd. All rights reserved.

1. INTRODUCTION

The finite element method [1] is regarded as the most accurate and versatile analysis tool specifically in structural analysis problems. The plate bending is one of the first problems where finite element was applied in the early 1960s. The initial attempts were made with thin plates based on Kirchhoff's hypothesis where a number of difficulties were encountered. These are mostly concerned with the satisfaction of normal slope continuity along the element edges. Subsequently, the method has been applied to thick plates based on Reissner–Mindlin's hypothesis where the above-mentioned continuity problem has been avoided by considering the transverse displacement (w) and rotations of normal (θ_x and θ_y) as independent displacement components. Amongst the thick plate elements developed so far, the most prominent elements are the isoparametric elements, which became very popular. Although these elements are quite elegant but they involve certain problems such

0022-460X/02/$35.00 © 2002 Elsevier Science Ltd. All rights reserved.

as shear locking, stress extrapolation, spurious modes and something else. Keeping these aspects in view, some research workers have tried to develop elements, which will be free from the above problems. The necessity has been geared up further with the wide use of fibre-reinforced laminated composites where the effect of shear deformation is more important. As an outcome of these facts, a number of thick plate elements have been proposed by different investigators such as Petrolito [2], Yuan and Miller [3], Sengupta [4], Batoz and Katili [5], Zhongnian [6] and a few others. In this group, the element, proposed by the last author of this paper [4], is quite powerful, which has been applied to free vibration analysis of plates with necessary additions and modifications in this paper. It is a high-precision element and it has the advantage that plates of any shapes can be modelled by this element, as it has a triangular geometry.

In this element, a fourth order complete polynomial has been used to express w while both θ_x and θ_y have been expressed with complete cubic polynomials. Thus the interpolation function of w is one order higher than those of θ_x and θ_y, which has helped to make this element free from shear locking and other relevant problems. The 35 constants of these three approximating polynomials have been expressed in terms of 35 nodal displacements of the element as shown in Figure 1. Thus the stiffness matrix of an element will have an order of 35, which has been reduced to 30 by eliminating the degrees of freedom of the internal node through static condensation. To perform the condensation, the mass of an element is lumped at its external nodes. The distribution of mass at the different nodes is made in proportion to the quantities obtained at the corresponding diagonals of the consistent mass matrix. The concept is somewhat similar to that of Hinton *et al.* [7]. In one of the mass lumping schemes, the contribution of rotary inertia has also been taken into account.

The formulation presented by Sengupta [4] has been followed with some modifications. Sengupta [4] has presented the stiffness matrix explicitly, which is quite elegant in its use but it cannot be used in a slightly different problem such as composite plate, tapered plates or something else. To eliminate these limitations, the integration of the stiffness matrix has been carried out numerically following Gauss quadrature technique. Moreover, the trouble taken by Sengupta [4] to express the 35 constants of the approximating polynomials in terms of 35 nodal unknowns has been avoided through a matrix inversion, which is quite easy to execute in a computer.

The element has been applied to free vibration analysis of plates having different boundary conditions, shapes and thickness ratios. It has also been tested with plates with internal opening and concentrated mass. The natural frequencies obtained in the present

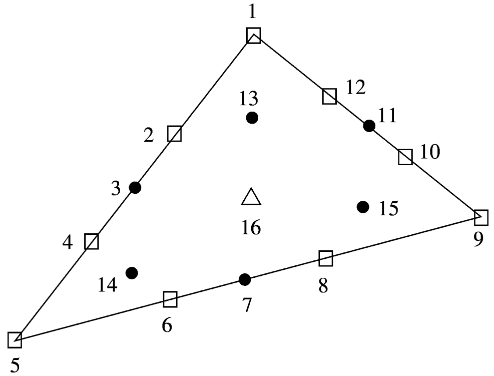

Figure 1. A typical element with all the nodes: ●, w; △, θ_x, θ_y; □, w, θ_x, θ_y.

analysis have been compared with those available in literature. The comparison shows the potentiality of the element in such a wide range of problems.

2. FORMULATION

The formulation is based on Reissner–Mindlin's plate theory, which ensures the incorporation of shear deformation. The scope of the work has been kept limited within linear analysis where the material of the plate has been assumed to be homogeneous and isotropic. The middle plane of the plate has been taken as the reference plane.

The formulation has been made in area co-ordinate system. In this system, the co-ordinate at any point p within a triangle (Figure 2) is expressed by L_1, L_2 and L_3, which may be defined as

$$L_i = A_i/\Delta \quad (i = 1, 2, 3),$$

where Δ is the area of the triangle $(A_1 + A_2 + A_3)$.

The relationship between area co-ordinates and rectangular co-ordinates is as follows:

$$x = L_1 x_1 + L_2 x_2 + L_3 x_3, \qquad y = L_1 y_1 + L_2 y_2 + L_3 y_3, \tag{1}$$

where

$$L_i = (a_i + b_i x + c_i y)/2\Delta \qquad (i = 1, 2, 3),$$

$$a_i = x_j y_k - x_k y_j,\ b_i = y_j - y_k \quad \text{and} \quad c_i = x_k - x_j.$$

The parameters i, j and k follow cyclic order of 1, 2 and 3. Using the above quantities, the area of the triangle may be defined as

$$\Delta = (a_1 + a_2 + a_3)/2.$$

Figure 1 shows a typical element, which has a total number of nodes equal to 16. The locations of nodes 3, 7 and 11 are the centres of the corresponding sides while the other

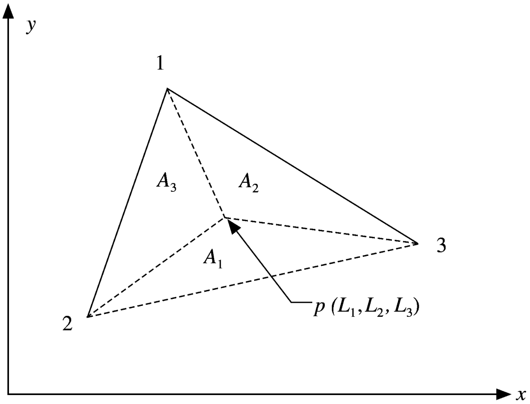

Figure 2. Area co-ordinate of a point within a triangle.

mid-side nodes (2, 4, 6, 8, 10 and 12) are located at a distance of one-third of the corresponding sides. The co-ordinates of the internal nodes 13, 14, 15 and 16 are (1/2, 1/4, 1/4), (1/4, 1/2, 1/4), (1/4, 1/4, 1/2) and (1/3, 1/3, 1/3) respectively. The degrees of freedom taken at all the external nodes (1–12) except 3, 7 and 11 are w, θ_x and θ_y while it is only w at nodes 3, 7, 11, 13, 14 and 15. For the centroidal node i.e., 16, it is θ_x and θ_y.

The transverse displacement (w) and rotations of normal (θ_x and θ_y) have been taken as the independent field variables, which are approximated as

$$w = [Q_w]\{\gamma\}, \qquad \theta_x = [Q_\theta]\{\mu\} \quad \text{and} \quad \theta_y = [Q_\theta]\{\lambda\}, \tag{2a–c}$$

where

$$[Q_w] = [L_1^4\ L_2^4\ L_3^4\ L_1^3L_2\ L_2^3L_1\ L_2^3L_3\ L_3^3L_2\ L_3^3L_1\ L_1^3L_3\ L_1^2L_2^2\ L_2^2L_3^2\ L_3^2L_1^2$$
$$L_1^2L_2L_3\ L_1L_2^2L_3\ L_1L_2L_3^2],$$

$$[Q_\theta] = [L_1^3\ L_2^3\ L_3^3\ L_1^2L_2\ L_2^2L_1\ L_2^2L_3\ L_3^2L_2\ L_3^2L_1\ L_1^2L_3\ L_1L_2L_3],$$

$$\{\gamma\} = [\gamma_1\ \gamma_2\ \gamma_3\ \gamma_4\ \gamma_5\ \gamma_6\ \gamma_7\ \gamma_8\ \gamma_9\ \gamma_{10}\ \gamma_{11}\ \gamma_{12}\ \gamma_{13}\ \gamma_{14}\ \gamma_{15}]^{\mathrm{T}},$$

$$\{\mu\} = [\mu_1\ \mu_2\ \mu_3\ \mu_4\ \mu_5\ \mu_6\ \mu_7\ \mu_8\ \mu_9\ \mu_{10}]^{\mathrm{T}},$$

$$\{\lambda\} = [\lambda_1\ \lambda_2\ \lambda_3\ \lambda_4\ \lambda_5\ \lambda_6\ \lambda_7\ \lambda_8\ \lambda_9\ \lambda_{10}]^{\mathrm{T}}.$$

The above equations (2a–c) have been appropriately substituted at the different nodes, which gives the relationship between the unknown constants of equations (2a–c) and the nodal degrees of freedom as

$$\{X\} = [A]\{\alpha\}, \tag{3}$$

where

$$\{\alpha\} = [[\gamma]^{\mathrm{T}}\ [\mu]^{\mathrm{T}}\ [\lambda]^{\mathrm{T}}]^{\mathrm{T}},$$

$$\{X\}^{\mathrm{T}} = [w_1\ \theta_{x1}\ \theta_{y1}\ w_2\ \theta_{x2}\ \theta_{y2}\ w_3\ w_4\ \theta_{x4}\ \theta_{y4}\ w_5\ \theta_{x5}\ \theta_{y5}\ w_6\ \theta_{x6}\ \theta_{y6}\ w_7\ w_8\ \theta_{x8}\ \theta_{y8}$$
$$w_9\ \theta_{x9}\ \theta_{y9}\ w_{10}\ \theta_{x10}\ \theta_{y10}\ w_{11}\ w_{12}\ \theta_{x12}\ \theta_{y12}\ w_{13}\ w_{14}\ w_{15}\ \theta_{x16}\ \theta_{y16}]$$

and the matrix $[A]$ contains the co-ordinates of the different nodes.

As θ_x and θ_y have been taken as the independent field variables and they are not the derivatives of w, the effect of shear deformation can be easily incorporated as

$$\begin{Bmatrix} \phi_x \\ \phi_y \end{Bmatrix} = \begin{Bmatrix} \theta_x - \partial w/\partial x \\ \theta_y - \partial w/\partial y \end{Bmatrix}, \tag{4}$$

where ϕ_x and ϕ_y are the average shear strain over the entire plate thickness and θ_x and θ_y are the total rotations of the normal.

The generalized stress–strain relationship of the plate may be expressed as

$$\{\sigma\} = [D]\{\varepsilon\}, \tag{5}$$

where the stress resultant vector $\{\sigma\}$ is

$$\{\sigma\} = [M_x \;\; M_y \;\; M_{xy} \;\; Q_x \;\; Q_y]. \tag{6}$$

The generalized strain vector $\{\varepsilon\}$ in terms of displacement field is

$$\{\varepsilon\} = \begin{Bmatrix} -\,\partial\theta_x/\partial x \\ -\,\partial\theta_y/\partial y \\ -\,\partial\theta_x/\partial y - \partial\theta_y/\partial x \\ \partial w/\partial x - \theta_x \\ \partial w/\partial y - \theta_y \end{Bmatrix} \tag{7}$$

and the rigidity matrix $[D]$ is

$$[D] = \begin{bmatrix} D_{11} & D_{12} & 0 & 0 & 0 \\ D_{12} & D_{22} & 0 & 0 & 0 \\ 0 & 0 & D_{33} & 0 & 0 \\ 0 & 0 & 0 & D_{44} & 0 \\ 0 & 0 & 0 & 0 & D_{55} \end{bmatrix}. \tag{8}$$

For isotropic material, the different quantities of the rigidity matrix (8) are

$$D_{11} = D_{22} = Eh^3/12(1 - v^2), \quad D_{12} = D_{21} = vD_{11}, \quad D_{33} = (1 - v)D_{11}/2$$

$$\text{and } D_{44} = D_{55} = Ehk/2(1 + v),$$

where k is the shear correction factor, which has been taken as 5/6 in all the cases.

Now, the field variables as defined in equation (2) may be substituted in the generalized strain vector $\{\varepsilon\}$ as expressed in equation (7), which leads to

$$\{\varepsilon\} = [C]\{\alpha\}, \tag{9}$$

where matrix $[C]$ contains L_i as appeared in equation (2) and their derivatives with respect to x and y.

The derivative with respect to, say x of any quantity, say $f(L_i)$ in the matrix $[C]$ has been carried out as follows:

$$\partial f(L_i)/\partial x = \{\partial f(L_i)/\partial L_1\}\{\partial L_1/\partial x\} + \{\partial f(L_i)/\partial L_2\}\{\partial L_2/\partial x\} + \{\partial f(L_i)/\partial L_3\}\{\partial L_3/\partial x\},$$

where $\partial L_i/\partial x$ can be evaluated with the help of equation (1).

Combining equations (3) and (9), the generalized strain vector $\{\varepsilon\}$ may be expressed as

$$\{\varepsilon\} = [B]\{X\}, \tag{10}$$

where

$$[B] = [C][A]^{-1}.$$

Once the matrices $[B]$ and $[D]$ are obtained, the element stiffness matrix $[K_e]$ can be derived with the help of Virtual work technique and it may be expressed as

$$[K_e] = \int_A [B]^{\mathrm{T}}[D][B]\,\mathrm{d}x\,\mathrm{d}y. \tag{11}$$

In a similar manner, the consistent mass matrix of an element can be derived and it may be expressed with the help of equations (2a–3) as

$$[M_{ec}] = \rho h\left(\int_A [A]^{-\mathrm{T}}[Q_1]^{\mathrm{T}}[Q_1][A]^{-1}\,\mathrm{d}x\,\mathrm{d}y + \frac{h^2}{12}\int_A [A]^{-\mathrm{T}}[Q_2]^{\mathrm{T}}[Q_2][A]^{-1}\,\mathrm{d}x\,\mathrm{d}y \right.$$
$$\left. + \frac{h^2}{12}\int_A [A]^{-\mathrm{T}}[Q_3]^{\mathrm{T}}[Q_3][A]^{-1}\,\mathrm{d}x\,\mathrm{d}y\right), \tag{12}$$

where

$$[Q_1] = [[Q_w]\ \ [N_2]\ \ [N_2]] \quad ([N_2] \text{ is a null matrix of order } 1\times 10),$$

$$[Q_2] = [[N_1]\ \ [Q_\theta]\ \ [N_2]] \quad ([N_1] \text{ is a null matrix of order } 1\times 15),$$

$$[Q_3] = [[N_1]\ \ [N_2]\ \ [Q_\theta]].$$

The first term of the mass matrix (12) is associated with transverse movement of mass, which is usually found to contribute the major inertia while the last two terms are associated with rotary inertia and their contribution becomes significant only in a plate having higher thickness ratio.

The consistent mass matrix presented above cannot be used in the present analysis, as it contributes sufficient amount of mass at the degrees of freedom of the internal nodes, which are to be eliminated through static condensation. Moreover, it is a populated matrix having off-diagonal terms, which connect the degrees of freedom of internal and external nodes. The above problem has been avoided by using a lumped mass matrix where the mass of an element has been distributed at its external nodes only. In this context three different mass lumping schemes have been recommended, which are as follows.

In the first lumping scheme, the mass has been taken at the degrees of freedom w of all the external nodes (see Figure 1). Thus the mass matrix contains 12 non-zero elements at 12 diagonals and their summation is equal to the mass of the element. The distribution of mass of an element at these 12 degrees of freedom has been made in proportion to the quantities obtained at the corresponding diagonal elements of the consistent mass matrix (12). The idea is similar to that of Hinton *et al.* [7] except that the mass at some of the nodes has not been taken in the present case. This mass lumping scheme has been defined as LS12. In the second lumping scheme, the mass of an element has been distributed at its nine external nodes having w, θ_x and θ_y as the degrees of freedom on the basis followed in LS12 (see Figure 1). Thus the central mid-side nodes, i.e., 3, 7 and 11 have not been considered in this case. This lumping scheme has been defined as LS9. The third lumping scheme is identical to LS9 with some addition to include the contribution of rotary inertia, which has not been taken in LS12 and LS9. The additional mass for the rotary inertia has been taken at the degrees of freedom θ_x and θ_y of those nine nodes. At any node, the mass taken at θ_x is identical to that at θ_y and it is equal to the mass at w multiplied by $h^2/12$. This quantity of

TABLE 1

Frequency parameters $\lambda = \omega a^2 \sqrt{(\rho h/D)}$ of a simply supported square plate

		Mode numbers					
h/a	References	1	2	3	4	5	6
0·01	LS12† (4 × 4)‡	19·735	49·326	49·351	79·168	98·669	98·682
	LS12 (5 × 5)	19·734	49·314	49·314	78·937	98·579	98·580
	LS12 (6 × 6)	19·734	49·313	49·313	78·884	98·556	98·556
	LS12 (8 × 8)	19·734	49·312	49·312	78·867	98·552	98·552
	LS12 (10 × 10)	19·734	49·312	49·312	78·866	98·552	98·552
	% Error§	00·010	00·182	00·182	00·030	00·035	00·036
	LS9¶ (4 × 4)	19·735	49·332	49·352	79·172	98·787	98·787
	LS9 (5 × 5)	19·734	49·315	49·321	78·986	98·654	98·654
	LS9 (6 × 6)	19·734	49·314	49·314	78·887	98·569	98·569
	LS9 (8 × 8)	19·734	49·313	49·313	78·869	98·556	98·556
	LS9 (10 × 10)	19·734	49·313	49·313	78·867	98·555	98·555
	% Error	00·010	00·182	00·182	00·030	00·036	00·036
	LS9RI‖ (4 × 4)	19·733	49·332	49·342	79·146	98·746	98·746
	LS9RI (5 × 5)	19·732	49·307	49·311	78·914	98·570	98·571
	LS9RI (6 × 6)	19·732	49·304	49·304	78·861	98·529	98·529
	LS9RI (8 × 8)	19·732	49·303	49·303	78·832	98·516	98·516
	LS9RI (10 × 10)	19·732	49·303	49·303	78·821	98·515	98·515
	% Error	00·000	00·000	00·000	00·026	00·002	00·002
	Mindlin's solution [9]	19·732	49·303	49·303	78·842	98·517	98·517
	LS12 (5 × 5)	19·195	46·065	46·065	70·837	86·268	86·268
0·1	LS12 (6 × 6)	19·198	46·106	46·106	70·883	86·545	86·546
	LS12 (8 × 8)	19·201	46·146	46·146	71·129	86·818	86·819
	LS12 (10 × 10)	19·202	46·161	46·161	71·216	86·983	86·984
	% Error	00·718	1·493	1·493	2·037	2·287	2·287
	LS9 (5 × 5)	19·198	46·107	46·107	70·994	86·564	86·564
	LS9 (6 × 6)	19·200	46·134	46·134	71·089	86·742	86·742
	LS9 (8 × 8)	19·202	46·162	46·162	71·188	86·925	86·925
	LS9 (10 × 10)	19·203	46·175	46·175	71·213	87·143	87·143
	% Error	00·718	1·527	1·527	2·037	2·475	2·475
	LS9RI (5 × 5)	19·058	45·398	45·398	69·502	84·506	84·506
	LS9RI (6 × 6)	19·060	45·423	45·423	69·585	84·659	84·659
	LS9RI (8 × 8)	19·062	45·449	45·449	69·674	84·821	84·821
	LS9RI (10 × 10)	19·062	45·462	45·462	69·734	84·985	84·985
	% Error	00·015	00·044	00·044	00·086	00·062	00·062
	Mindlin's solution [9]	19·065	45·482	45·482	69·794	85·038	85·038
0·2	LS12 (5 × 5)	17·799	39·130	39·130	56·252	66·019	66·019
	LS12 (6 × 6)	17·809	39·230	39·230	56·551	66·514	66·514
	LS12 (8 × 8)	17·818	39·330	39·330	56·852	67·010	67·010
	LS12 (10 × 10)	17·830	39·376	39·376	57·008	67·241	67·241
	% Error	2·189	3·208	3·208	3·369	3·217	3·217
	LS9 (5 × 5)	17·809	39·230	39·231	56·558	66·521	66·521
	LS9 (6 × 6)	17·815	39·299	39·299	56·762	66·860	66·860
	LS9 (8 × 8)	17·822	39·369	39·369	56·971	67·206	67·206
	LS9 (10 × 10)	17·833	39·378	39·378	57·092	67·287	67·287
	% Error	2·189	3·208	3·208	3·521	3·288	3·288

TABLE 1

Continued

h/a	References	Mode numbers 1	2	3	4	5	6
	LS9RI (5 × 5)	17·429	37·954	37·954	54·567	64·186	64·186
	LS9RI (6 × 6)	17·435	38·014	38·014	54·846	64·646	64·646
	LS9RI (8 × 8)	17·442	38·074	38·074	54·966	64·841	64·841
	LS9RI (10 × 10)	17·444	38·102	38·102	55·000	64·898	64·898
	% Error	00·023	00·131	00·131	00·272	00·379	00·379
	Mindlin's solution [9]	17·448	38·152	38·152	55·150	65·145	65·145
2·5	LS12 (5 × 5)	16·932	35·589	35·589	49·777	57·662	57·662
	LS12 (6 × 6)	16·944	35·708	35·708	50·103	58·179	58·179
	LS12 (8 × 8)	16·957	35·826	35·826	50·430	58·699	58·699
	LS12 (10 × 10)	16·964	35·996	35·996	50·612	59·102	59·102
	% Error	2·768	3·839	3·839	3·319	3·228	3·228
	LS9 (5 × 5)	16·944	35·707	35·708	50·105	57·752	57·752
	LS9 (6 × 6)	16·953	35·789	35·790	50·331	58·293	58·293
	LS9 (8 × 8)	16·962	35·872	35·872	50·561	58·789	58·789
	LS9 (10 × 10)	16·971	36·025	36·025	50·693	59·253	59·263
	% Error	2·811	3·923	3·923	3·484	3·491	3·496
	LS9RI (5 × 5)	16·481	34·434	34·434	48·347	55·537	55·537
	LS9RI (6 × 6)	16·489	34·504	34·504	48·537	56·027	56·027
	LS9RI (8 × 8)	16·497	34·574	34·574	48·730	56·612	56·612
	LS9RI (10 × 10)	16·503	34·602	34·602	48·842	57·125	57·125
	% Error	00·024	00·182	00·182	0·294	0·225	0·225
	Mindlin's solution [9]	16·507	34·665	34·665	48·986	57·254	57·254
Thin plate solution [10]		19·739	49·348	49·348	78·957	98·696	98·696

†Present analysis using mass lumping scheme LS12.
‡Quantity with the parentheses indicates mesh size.
§Percentage error is calculated taking Mindlin's solution [9] as the basis.
¶Present analysis using mass lumping scheme LS9.
‖Present analysis using mass lumping scheme LS9RI.
These are followed in other tables also.

mass taken at θ_x and θ_y for rotary inertia may be justified with the expression of consistent mass matrix presented in equation (12). Although $[Q_\theta]$ is different from $[Q_w]$ it will not make a major difference since the consistent mass matrix is utilized to get the distribution ratio of the mass without changing its total quantity.

Based on the above discussion, it is clear that the computation of the consistent mass matrix (12) is necessary only for its first term. The integration associated with this and the stiffness matrix (11) has been carried out numerically following Gauss quadrature technique.

Following any one of the above lumping schemes, the mass matrix can be formed, which will be a diagonal matrix having zero mass at the degrees of freedom of the internal nodes. With such a mass matrix, it is easy to perform the condensation mentioned earlier.

The stiffness matrix and mass matrix having an order of 30 in their final form have been evaluated for all the elements and they have been assembled together to form the overall

TABLE 2

Frequency parameters $\lambda = \omega a^2 \sqrt{(\rho h/D)}$ of a square plate having two opposite edges simply supported and the other two edges free

h/a	References	Mode number 1	2	3	4	5	6
0·001	LS9RI (4 × 4)	9·620	15·998	35·875	38·832	46·313	69·403
	LS9RI (5 × 5)	9·623	16·047	36·176	38·872	46·457	69·845
	LS9RI (6 × 6)	9·626	16·073	36·339	38·894	46·539	70·099
	LS9RI (7 × 7)	9·627	16·083	36·440	38·907	46·590	70·260
	LS9RI (8 × 8)	9·628	16·100	36·506	38·916	46·624	70·368
	LS9RI (10 × 10)	9·629	16·112	36·584	38·926	46·664	70·497
	Liew *et al.* [11]	9·640	16·142	36·729	38·947	46·739	70·739
	LS9RI (4 × 4)	9·429	15·271	33·105	36·177	42·285	60·678
0·1	LS9RI (5 × 5)	9·433	15·310	33·366	36·241	42·460	61·178
	LS9RI (6 × 6)	9·435	15·333	33·510	36·276	42·557	61·459
	LS9RI (7 × 7)	9·436	15·347	33·599	36·297	42·617	61·633
	LS9RI (8 × 8)	9·437	15·356	33·659	36·310	42·656	61·748
	LS9RI (10 × 10)	9·438	15·367	33·729	36·327	42·704	61·888
	Liew *et al.* [11]	9·440	15·389	33·859	36·357	42·792	62·149
	LS9RI (4 × 4)	8·967	13·966	28·476	31·005	35·389	48·150
0·2	LS9RI (5 × 5)	8·973	14·010	28·708	31·100	35·589	48·636
	LS9RI (6 × 6)	8·976	14·035	28·836	31·152	35·700	48·909
	LS9RI (7 × 7)	8·978	14·050	28·915	31·183	35·768	49·078
	LS9RI (8 × 8)	8·979	14·060	28·966	31·203	35·812	49·189
	LS9RI (10 × 10)	8·980	14·073	29·027	31·227	35·865	49·322
	Liew *et al.* [11]	8·983	14·093	29·136	31·270	35·960	49·561
Thin plate solution [10]		9·631	16·135	36·726	38·945	46·738	70·740

stiffness matrix $[K_s]$ and mass matrix $[M_s]$, respectively. The storage of $[K_s]$ and $[M_s]$ has been done in single array following skyline storage technique with proper care for the different degrees of freedom at the different nodes. Once $[K_s]$ and $[M_s]$ are obtained, the equation of motion of the plate may be expressed as

$$[K_s]\{X_s\} = \omega^2 [M_s]\{X_s\}. \tag{13}$$

After incorporating the boundary conditions, the above equation has been solved by simultaneous iterative technique [8] to get frequency ω for the first few modes.

3. NUMERICAL EXAMPLES

In this section, numerical examples of plates have been solved by the high-precision element and the results obtained have been compared with the published results in all the cases. The examples cover a wide range of problems, which include different plate shapes, boundary conditions, thickness ratios, cutouts and concentrated masses at the plate centre.

TABLE 3

Frequency parameters $\lambda = \omega b^2\sqrt{(\rho h/D)}$ of a clamped rectangular plate

			Mode number					
h/a	b/a	References	1	2	3	4	5	6
0·01	1·0	LS12 (4 × 4)	36·025	73·558	73·773	110·145	136·304	136·352
		LS12 (6 × 6)	35·955	73·301	73·326	108·232	131·465	132·108
		LS12 (8 × 8)	35·947	73·262	73·262	107·976	131·223	131·859
		Leissa [10]	35·992	73·413	73·413	108·270	131·640	132·240
	1·5	LS12 (6 × 4)	60·676	93·798	148·72	149·912	180·343	228·130
		LS12 (9 × 6)	60·635	93·587	148·22	149·165	178·838	225·837
		LS12 (12 × 8)	60·633	93·573	148·19	149·116	178·738	225·693
		Leissa [10]	60·772	93·860	148·82	149·740	179·660	226·920
	2·5	LS12 (10 × 4)	147·71	173·81	221·61	292·463	386·089	394·701
		LS12 (15 × 6)	147·67	173·66	221·18	291·444	383·992	393·709
		LS12 (20 × 8)	147·66	173·65	221·15	291·379	383·849	393·645
		Leissa [10]	147·80	173·85	221·54	291·890	384·710	394·370
0·1	1·0	LS9RI (4 × 4)	32·480	61·692	61·705	86·107	100·785	101·693
		LS9RI (6 × 6)	32·503	61·887	61·887	86·544	101·751	102·705
		LS9RI (8 × 8)	32·512	61·953	61·953	86·718	102·049	103·015
		Liew *et al.* [11]	32·524	62·038	62·034	86·949	102·435	103·412
	1·5	LS9RI (6 × 4)	56·018	84·177	126·77	128·845	149·833	185·257
		LS9RI (9 × 6)	56·043	84·258	127·13	129·161	150·333	186·264
		LS9RI (12 × 8)	56·052	84·288	127·24	129·276	150·516	186·616
		Liew *et al.* [11]	56·065	84·329	127·39	129·429	150·758	187·079
	2·5	LS9RI (10 × 4)	137·206	160·05	201·43	261·046	336·483	337·707
		LS9RI (15 × 6)	137·261	160·12	201·57	261·357	337·173	338·626
		LS9RI (20 × 8)	137·278	160·16	201·63	261·413	337·348	338·852
		Liew *et al.* [11]	137·305	160·19	201·69	261·637	337·793	339·286

3.1. RECTANGULAR PLATES

As a first case, a simply supported square plate has been analyzed with different mesh divisions using the different mass lumping schemes mentioned earlier. The study has been made for different values of thickness ratio (h/a) ranging from 0·01 to 0·25. The first six frequencies obtained in all the cases have been presented in Table 1 with the analytical solution of Mindlin [9] and Leissa [10], where the results of Leissa [10] are based on classical plate theory. Taking Mindlin's thick plate solution [9] as the exact one, the % error has been calculated in all the cases and presented in Table 1. The table shows that the % error is less than 0·4% for any thickness ratio when mass lumping scheme LS9RI is used while it is more than 3% for higher thickness ratios when LS12 and LS9 are used. This is due to the effect of rotary inertia (mentioned in the previous section), which became significant in plates of higher thickness ratio, as expected. As the contribution of rotary inertia is not significant in thin plates, the mass lumping schemes LS12 and LS9 have

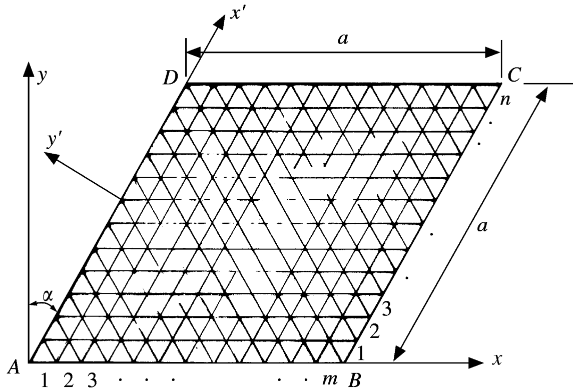

Figure 3. A skew plate having a mesh division of $m \times n$.

TABLE 4

Frequency parameters $\lambda = \omega a^2 \sqrt{(\rho h/D)}$ *of a skew plate*

Skew angle	References	Mode number 1	2	3	4	5	6
All edges simply supported							
30°	LS12 (6 × 6)	25·110	52·570	72·100	83·720	122·25	121·903
	LS12 (7 × 7)	25·065	52·584	72·023	83·752	122·41	122·427
	LS12 (8 × 8)	25·032	52·590	71·959	83·761	122·49	122·500
	LS12 (10 × 10)	24·990	52·765	71·868	83·760	122·56	122·540
	Liew and Lam [12]	25·069	52·901	72·344	84·780	130·25	
45°	LS12 (6 × 6)	35·850	66·168	100·30	109·19	139·99	167·13
	LS12 (7 × 7)	35·700	66·189	100·32	108·86	140·24	167·48
	LS12 (8 × 8)	35·560	66·203	100·31	108·59	140·36	167·64
	LS12 (10 × 10)	33·563	66·209	100·28	108·21	140·45	167·78
	Liew and Lam [12]	34·938	66·422	100·87	107·78	175·28	
60°	LS12 (6 × 6)	67·309	104·62	148·39	194·16	214·10	245·15
	LS12 (7 × 7)	66·689	104·70	148·27	194·97	213·23	246·95
	LS12 (8 × 8)	66·208	104·74	148·25	195·31	212·51	247·66
	LS12 (10 × 10)	66·517	104·77	148·15	195·57	211·65	248·13
	Barik [13]	66·345	104·64	147·84	194·14	213·67	245·78
All edges clamped							
30°	LS12 (6 × 6)	46·001	81·313	104·69	118·55	163·30	163·63
	LS12 (7 × 7)	46·016	81·365	104·78	118·71	163·81	164·15
	LS12 (8 × 8)	46·020	81·389	104·82	118·79	164·04	164·38
	LS12 (10 × 10)	46·022	81·409	104·86	118·85	164·22	164·57
	Durvasula [14]	46·140	81·691	105·51	119·52	165·80	
45°	LS12 (6 × 6)	65·487	105·98	147·19	156·23	194·23	226·10
	LS12 (7 × 7)	65·495	106·07	147·45	156·37	195·03	227·14
	LS12 (8 × 8)	65·500	106·12	147·57	156·46	195·37	227·61
	LS12 (10 × 10)	65·506	106·16	147·67	156·54	195·64	227·99
	Durvasula [14]	65·929	106·59	149·03	158·90	199·37	231·94
60°	LS12 (6 × 6)	121·06	176·19	228·41	282·40	300·83	345·80
	LS12 (7 × 7)	121·10	176·34	229·22	286·55	301·18	346·17
	LS12 (8 × 8)	121·13	176·54	229·65	287·82	301·54	348·59
	LS12 (10 × 10)	121·16	176·70	230·03	288·75	302·00	350·41
	Mizusawa *et al.* [15]	120·90	177·75	231·74	292·54	301·81	357·58

TABLE 5

Frequency parameters $\lambda = \omega a^2 \sqrt{(\rho h/D)}$ of a simply supported skew plate

h/a	Skew angle	References	Mode number 1	2	3	4	5	6
	30°	LS9RI (6 × 6)	23·867	47·967	63·406	72·549	99·792	99·822
		LS9RI (7 × 7)	23·866	48·056	63·596	72·858	100·652	100·665
		LS9RI (8 × 8)	23·865	48·111	63·711	73·049	101·181	101·185
		LS9RI (10 × 10)	23·865	48·174	63·839	73·265	101·777	101·776
0·1	45°	LS9RI (6 × 6)	33·039	59·183	85·006	90·331	112·354	129·193
		LS9RI (7 × 7)	33·015	59·304	85·359	90·689	113·228	130·542
		LS9RI (8 × 8)	32·994	59·379	85·578	90·906	113·769	131·378
		LS9RI (10 × 10)	32·962	59·466	85·826	91·140	114·384	132·331
	60°	LS9RI (6 × 6)	57·759	88·795	118·21	147·29	154·969	175·419
		LS9RI (7 × 7)	57·679	89·059	118·82	148·66	156·090	177·893
		LS9RI (8 × 8)	57·608	89·224	119·19	149·48	156·798	179·354
		LS9RI (10 × 10)	57·495	89·411	119·61	150·39	157·590	180·957
	30°	LS9RI (6 × 6)	21·371	39·537	49·953	55·810	71·942	71·974
		LS9RI (7 × 7)	21·392	39·712	50·308	56·316	73·104	73·118
		LS9RI (8 × 8)	21·404	39·825	50·535	56·693	73·854	73·860
		LS9RI (10 × 10)	21·418	39·956	50·799	57·027	74·734	74·736
0·2	45°	LS9RI (6 × 6)	28·595	47·381	63·833	66·950	79·693	88·812
		LS9RI (7 × 7)	28·618	47·604	64·389	67·568	80·837	90·433
		LS9RI (8 × 8)	28·630	47·748	64·748	67·967	81·577	91·486
		LS9RI (10 × 10)	28·638	47·915	65·169	68·429	82·449	92·731
	60°	LS9RI (6 × 6)	46·328	66·647	83·851	99·735	103·51	114·04
		LS9RI (7 × 7)	46·394	67·047	84·666	101·26	104·93	116·51
		LS9RI (8 × 8)	46·427	67·304	85·192	102·21	105·88	118·05
		LS9RI (10 × 10)	46·448	67·605	85·807	103·33	107·00	119·82

performed well for thickness ratio $h/a = 0{\cdot}01$. Again LS12 has performed marginally better than LS9 and it is due to a better distribution of mass in LS12 over LS9. Based on these observations, LS9RI can be recommended for plates having any thickness while LS12 may be recommended for thin plates only.

Now a square plate having two opposite edges simply supported and the other two edges free has been studied taking $h/a = 0{\cdot}001$, 0·1, and 0·2. Using LS9RI, the analysis has been done with different mesh divisions and the first six frequencies obtained have been presented with the thin plate solution of Leissa [10] and thick plate solution of Liew *et al.* [11] in Table 2. The results show that the element performed well with LS9RI in the present problem.

Finally, a rectangular plate having all the side clamped has been analyzed with different mesh divisions. The study has been made for aspect ratio $a/b = 1{\cdot}0$, 1·5 and 2·5 where h/a has been taken as 0·01 and 0·1 in all the cases. The analysis has been performed with LS12 for $h/a = 0{\cdot}01$ and LS9RI for $h/a = 0{\cdot}1$. The results obtained in the present analysis have been presented with those of Leissa [10] ($h/a = 0{\cdot}01$) and Liew *et al.* [11] ($h/a = 0{\cdot}1$) in Table 3. The table shows that the present results agreed well with those of Leissa [10] and Liew *et al.* [11].

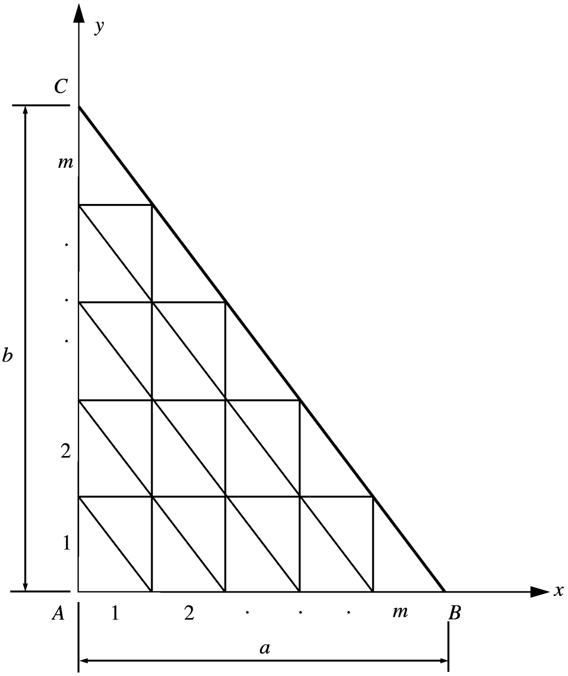

Figure 4. A triangular plate having a mesh division of $m \times m$.

3.2. SKEW PLATES

A skew plate as shown in Figure 3 has been studied for different skew angles (α) taking all the sides simply supported in one case while it is clamped in another case. As the sides BC and AD (Figure 3) are inclined to global axis system (x–y), necessary transformation has been made to express the degrees of freedom of the nodes on these two sides along x'–y' (Figure 3). The transformation has been done in element level. The thickness ratio of the plate is taken as 0·01. Using LS12, the plate has been analyzed with four different mesh divisions (Figure 3) in all the cases and the first six frequencies obtained have been compared with those of Liew and Lam [12], Barik [13], Durvasula [14] and Mizusawa *et al.* [15] in Table 4. In this group the finite element solution is due to Barik [13] who had to take a mesh division of 24×24 for skew angles of 30° and 45° while it is 36×36 for 60° skew angle. The present analysis has been done with a highest mesh division of 10×10, which give sufficiently good results compared to those of others [12–15].

Again the simply supported plate has been analysed for $h/a = 0{\cdot}1$ and $0{\cdot}2$ using LS9RI and the first six frequencies obtained have been presented in Table 5. The results are presented for the same skew angle and mesh divisions used in the previous case.

3.3. TRIANGULAR PLATES

A triangular plate as shown in Figure 4 simply supported at the three sides has been studied for different aspect ratios (b/a). Similar to the earlier case, necessary transformation has been made for the degrees of freedom of the nodes along the side BC (Figure 4). The plate has been analyzed with different mesh divisions (Figure 4) in all the cases and the first six frequencies obtained have been presented in Table 6. Taking thickness ratio of the plate

TABLE 6

Frequency parameters $\lambda = \omega a^2\sqrt{(\rho h/D)}$ of a triangular plate

b/a	References	Mode number 1	2	3	4	5	6
1·0	LS12 (5 × 5)	49·31	98·58	128·26	167·30	197·93	242·53
	LS12 6 × 6)	49·31	98·56	128·11	167·34	197·17	246·57
	LS12 (7 × 7)	49·31	98·55	128·07	167·35	196·95	246·88
	LS12 (8 × 8)	49·31	98·55	128·06	167·35	196·85	249·92
	Kim and Dickinson [16]	49·35	99·76	128·40	169·10	200·30	249·80
	Geannakakes [17]	49·34	98·69	128·30	167·80	197·46	246·86
1·5	LS12 (5 × 5)	34·27	65·55	91·78	107·88	138·61	157·62
	LS12 (6 × 6)	34·26	65·53	91·75	107·26	138·41	156·51
	LS12 (7 × 7)	34·26	65·53	91·75	107·22	138·95	158·86
	LS12 (8 × 8)	34·26	65·53	91·74	107·22	138·98	158·80
	Kim and Dickinson [16]	34·28	65·69	91·99	108·00	140·90	140·90
	Geannakakes [17]	34·28	65·59	91·86	107·48	139·39	162·42
2·0	LS12 (5 × 5)	27·76	49·80	73·41	80·62	108·70	120·23
	LS12 (6 × 6)	27·76	49·87	74·46	81·27	103·78	118·54
	LS12 (7 × 7)	27·75	49·86	74·62	81·27	105·68	119·76
	LS12 (8 × 8)	27·75	49·86	74·62	81·25	106·10	119·72
	Kim and Dickinson [16]	27·76	49·91	74·85	81·84	107·40	122·20
	Geannakakes [17]	27·76	49·88	74·88	81·51	108·43	121·65
2·5	LS12 (5 × 5)	24·16	40·88	59·58	71·50	87·37	102·77
	LS12 (6 × 6)	24·14	41·10	59·93	71·85	82·62	101·19
	LS12 (7 × 7)	24·14	41·11	60·49	71·82	82·16	102·35
	LS12 (8 × 8)	24·14	41·11	60·51	71·81	83·28	102·14
	Kim and Dickinson [16]	24·15	41·15	60·65	72·28	84·92	104·20
	Geannakakes [17]	24·15	41·14	61·14	71·99	86·49	103·66
3·0	LS12 (5 × 5)	21·83	35·35	50·21	64·99	66·54	93·22
	LS12 (6 × 6)	21·85	35·57	50·32	65·46	67·87	88·62
	LS12 (7 × 7)	21·85	35·61	50·96	66·05	68·21	87·88
	LS12 (8 × 8)	21·85	35·61	51·07	66·10	69·02	86·27
	Kim and Dickinson [16]	21.85	35·63	51·27	66·73	71·03	92·84
	Geannakakes [17]	21·84	35·65	52·15	66·67	73·97	94·15

as 0·01, the analysis has been done using LS12. The same problem has been studied by Kim and Dickinson [16] using the Rayleigh–Ritz method and also by Geannakakes [17] using the Rayleigh–Ritz method with normalized characteristic orthogonal polynomials. The results obtained by Kim and Dickinson [16] and Geannakakes [17] have also been presented in Table 6 for necessary comparison, which indicates the efficacy and accuracy of the present element.

3.4. A RECTANGULAR PLATE WITH A LUMPED MASS AT THE PLATE CENTRE

The vibration of a rectangular plate 0·71 m long, 0·42 m wide and 2·0 mm thick having a concentrated mass at the plate centre has been studied. The mass of the plate has also been considered in the analysis. The plate is simply supported at the two opposite sides having

TABLE 7

Fundamental frequencies ($\lambda = \omega/2\pi$) of a rectangular plate having a concentrated mass at the plate centre

Concentrated mass (kg)	Boay [18]	Present analysis mesh divisions		
		6×4	8×6	10×6
0·24	48·75	48·70	48·65	48·64
0·50	38·83	38·78	38·73	38·72
0·74	33·48	33·43	33·35	33·33
1·00	29·54	29·52	29·49	29·48
1·24	26·95	26·93	26·90	26·88
1·48	24·96	24·92	24·89	24·87
1·76	23·09	23·05	22·98	22·96
1·98	21·88	21·84	21·80	21·79
2·22	20·76	20·72	20·68	20·67
2·48	19·72	19·69	19·65	19·64
2·75	18·79	18·75	18·69	18·67
3·00	18·03	17·99	17·94	17·93
3·25	17·36	17·32	17·29	17·27
3·50	16·76	16·73	16·68	16·66
3·75	16·22	16·19	16·15	16·13
4·00	15·73	15·70	15·67	15·65
4·25	15·28	15·25	15·19	15·17
4·50	14·86	14·83	14·80	14·79
4·75	14·48	14·45	14·40	14·38
5·00	14·12	14·10	14·05	14·04

a length of 0·42 m while the other two sides are clamped. For a wide range of values of the concentrated mass, the plate has been analyzed with three different mesh divisions and the fundamental frequencies obtained have been presented with the Ritz solution of Boay [18] in Table 7. The results agreed well. The mass matrix used is in accordance with LS12. The material properties of the plate are: $E = 70{\cdot}0$ GPa, $\nu = 0{\cdot}3$ and $\rho = 2770\,\mathrm{kg/m^3}$.

3.5. A SQUARE PLATE WITH A CUTOUT AT THE PLATE CENTRE

A simply supported square plate having a rectangular cutout at the plate centre has been studied for different size and aspect ratio of the cutout taking $h/a = 0{\cdot}01$, $0{\cdot}1$ and $0{\cdot}2$. The edges of the cutout are free and they are parallel to the edges of the plate. The plate has been analyzed with a mesh size of 10×10 using LS12 for $h/a = 0{\cdot}01$ and LS9RI for $h/a = 0{\cdot}1$ and $0{\cdot}2$. The first four frequencies obtained in the present analysis have been presented in Table 8 with the Rayleigh quotient and finite element solution of Lee *et al.* [19] ($h/a = 00{\cdot}1$) for necessary comparison. The table shows that the present results are in better agreement with the finite element results of Lee *et al.* [19] compared to their analytical solution in general.

4. CONCLUSION

A high-precision shear deformable triangular element developed by one of the authors of this paper has been applied to free vibration analysis of plates with little additions and

TABLE 8

Frequency parameters $\lambda = \omega a^2 \sqrt{(\rho h/D)}$ of a simply supported square plate having a rectangular cutout at the plate centre

			Cutout size						
h/a	References	Mode number	$(0·2a)\times(0·2a)$	$(0·4a)\times(0·4a)$	$(0·6a)\times(0·6a)$	$(0·8a)\times(0·8a)$	$(0·4a)\times(0·2a)$	$(0·8a)\times(0·4a)$	$(0·6a)\times(0·2a)$
0·01	Present analysis (LS12)	1	19·13	20·72	28·23	56·14	19·06	23·49	18·88
		2	47·67	41·00	42·39	68·07	41·31	28·09	32·43
		3	47·67	41·00	42·39	68·07	46·74	55·33	47·67
		4	76·34	71·31	75·36	121·0	73·84	64·75	68·17
	Present analysis (LS9RI)	1	19·12	20·69	28·13	55·35	19·04	23·44	18·96
		2	47·68	40·97	42·21	67·08	41·30	28·04	32·37
		3	47·68	40·97	42·21	67·09	46·71	55·15	47·82
		4	76·32	71·27	75·13	119·4	73·83	64·63	68·61
	Lee *et al.* [19] (FEM)	1	19·12	20·73	28·24	57·45	19·01	23·58	18·98
		2	47·77	41·10	42·57	69·82	41·43	28·26	32·53
		3	47·77	41·10	42·57	69·82	46·58	55·64	47·81
		4	76·80	71·55	74·99	124·2	74·10	65·18	69·17
	Lee *et al.* [19] (Analytical)	1	18·90	20·55	28·49	58·84	18·98	23·80	19·11
		2	49·65	43·92	45·12	77·83	44·08	26·43	32·53
		3	49·65	43·92	45·12	77·83	46·91	55·83	47·81
		4	71·72	70·69	75·55	124·99	72·28	69·48	76·84
0·1	Present analysis (LS12)	1	18·65	20·13	27·07	50·27	18·50	22·28	18·33
		2	44·36	36·47	37·75	56·79	35·79	24·86	27·75
		3	45·42	36·53	37·80	56·85	42·91	51·25	44·61
		4	69·88	64·60	55·52	65·15	66·33	56·91	60·46
	Present analysis (LS9RI)	1	18·44	19·81	26·17	44·77	18·29	21·83	18·10
		2	42·77	35·84	36·47	50·57	35·39	24·41	27·44
		3	42·83	35·92	36·54	50·64	42·24	49·45	43·69
		4	67·52	63·95	53·59	58·03	65·03	55·48	59·35
0·2	Present analysis (LS12)	1	17·42	19·03	25·33	42·93	17·42	20·47	17·19
		2	37·05	30·89	32·46	45·05	29·39	21·60	23·09
		3	38·43	30·94	32·50	45·11	36·52	44·12	38·63
		4	56·07	51·19	43·29	47·51	53·39	46·63	48·53
	Present analysis (LS9RI)	1	16·98	18·11	22·86	31·04	16·82	19·26	16·53
		2	35·17	29·48	29·35	32·47	28·53	20·42	22·33
		3	35·22	29·55	29·40	32·52	35·19	40·36	36·76
		4	53·50	49·03	39·16	34·10	51·53	43·99	46·76

modifications in the element formulation. Some mass lumping schemes have been proposed, which may be considered as one of the most significant contributions of this paper. The concept regarding incorporation of mass for rotary inertia is really elegant, which may be used in other elements. The element has been tested with a wide variety of benchmark problems where it has been found that the performance of the element is excellent in most of the cases. Any problem such as shear locking or spurious mode has not been encountered even in the analysis of the plate having a thickness ratio (h/a) of 0·001. The potential of the element is clearly reflected by the order of accuracy in the present analysis and the variety of problems considered.

REFERENCES

1. O. C. ZIENKIEWICZ and R. L. TAYLOR 1988 *The Finite Element Method* (two volumes). New York: McGraw-Hill.
2. J. PETROLITO 1989 *Computers and Structures* **32**, 1303–1309. A modified ACM element for thick plate analysis.
3. F. G. YUAN and R. E. MILLER 1989 *International Journal of Numerical Methods and Engineering* **28**, 109–126. A cubic triangular finite element for flat plates with shear.
4. D. SENGUPTA 1991 *International Journal of Numerical Methods and Engineering* **32**, 1389–1409. Stress analysis of flat plates with shear using explicit stiffness matrix.
5. J. L. BATOZ and I. KATILI 1992 *International Journal of Numerical Methods and Engineering* **35**, 1603–1632. On a simple triangular Reissner/Mindlin plate element based on incompatible modes and discrete constraints.
6. XU. ZHONGNIAN 1992 *International Journal of Numerical Methods and Engineering* **33**, 963–973. A thick–thin triangular plate element.
7. E. HINTON, T. ROCK and O. C. ZIENKIEWICZ 1976 *Earthquake Engineering and Structural Dynamics* **4**, 245–249. A note on mass lumping and related processes in the finite element method.
8. R. B. CORR and A. JENNINGS 1976 *International Journal of Numerical Methods and Engineering* **10**, 647–663. A simultaneous iteration algorithm for symmetric eigenvalue problems.
9. R. D. MINDLIN 1951 *Journal of Applied Mechanics American Society of Mechanical Engineers* **18**, 31–38. Influence of rotary inertia and shear on flexural motions of isotropic, elastic plates.
10. W. LEISSA 1973 *Journal of Sound and Vibration* **31**, 257–293. The free vibration of rectangular plates.
11. K. M. LIEW, Y. XIANG and S. KITIPORNCHAI 1993 *Computers and Structures* **49**, 1–29. Transverse vibration of thick rectangular plates—1: comprehensive sets of boundary conditions.
12. K. M. LIEW and K. Y. LAM 1990 *Journal of Sound and Vibration* **139**, 241–252. Application of two dimensional orthogonal plate function of flexural vibration of skew plates.
13. M. BARIK 1999 *Ph.D. Thesis, Indian Institute of Technology, Kharagpur, India*. Finite element static, dynamic and stability analysis of arbitrary stiffened plates.
14. S. DURVASULA 1969 *American Institute of Aeronautics and Astronautics Journal* **7**, 1164–1167. Natural frequencies and modes of clamped skew plates.
15. T. MIZUSAWA, T. KAJIKA M. and NARUOKA 1979 *Journal of Sound and Vibration* **62**, 301–308. Vibration of skew plates by using b-spline function.
16. C. S. KIM and S. M. DICKINSON 1990 *Journal of Sound and Vibration* **141**, 291–311. The free flexural vibration of right triangular isotropic and orthotropic plates.
17. G. N. GEANNAKAKES 1995 *Journal of Sound and Vibration* **182**, 441–478. Natural frequencies of arbitrarily shaped plates using the Rayleigh–Ritz method together with natural coordinate regions and normalized characteristic orthogonal polynomials.
18. C. G. BOAY 1993 *Computers and Structures* **48**, 39–47. Frequency analysis of rectangular isotropic plates carrying a concentrated mass.
19. H. L. LEE, S. P. LIM and S. T. CHOW 1990 *Computers and structures* **36**, 861–869. Prediction of natural frequencies of rectangular plates with rectangular cutouts.